Final Report

DISTRIBUTION STATEMENT A. Approved for public release; distribution is unlimited.

Shelf Break Acoustics – NESBA and SCS Data Analysis

Dr. Ying-Tsong Lin
Applied Ocean Physics and Engineering Department
Woods Hole Oceanographic Institution, Woods Hole, MA 02543
phone: (508) 685-3209   fax: (508) 457-2194   email: ytlin@whoi.edu

Award Number: N00014-21-1-2959

INTRODUCTION

Sound propagation in the ocean can be affected by many environmental factors, including physical oceanography (PO), marine geology (GEO) and biology (BIO). The primary objective of this project is to investigate the physics link between acoustics and environment variabilities. The ocean processes of particular interest include shelf-break fronts, thermohaline intrusions, surface mixed layers, and internal waves (Lin et al., 2009; Lynch et al., 2010; Lin and Lynch, 2011; Duda et al., 2012; Lynch et al., 2012; Emerson et al., 2015) along with other significant marine geological features and biological factors, such as submarine canyons (Lin et al., 2015), seabed properties (Ballard et al., 2010; Ballard et al., 2019), and fish schooling and shoaling (Newhall et al., 2017). Data collected in the shelf break areas of the New England shelf (see Figure 1) and northern South China Sea (see Figure 2) were studied. These two experiments were supported by the ONR Task Force Ocean (TFO) Program. The research approach is employed to enhance theory development, numerical modeling and field work experiments with strong interdisciplinary collaborations.

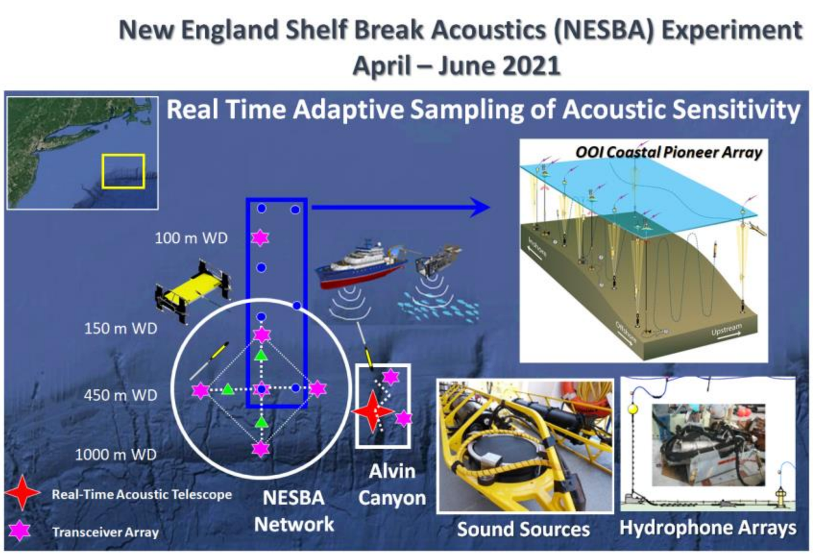

Figure 1. Equipment layout of the New England Shelf Break Acoustics (NESBA) Experiment.

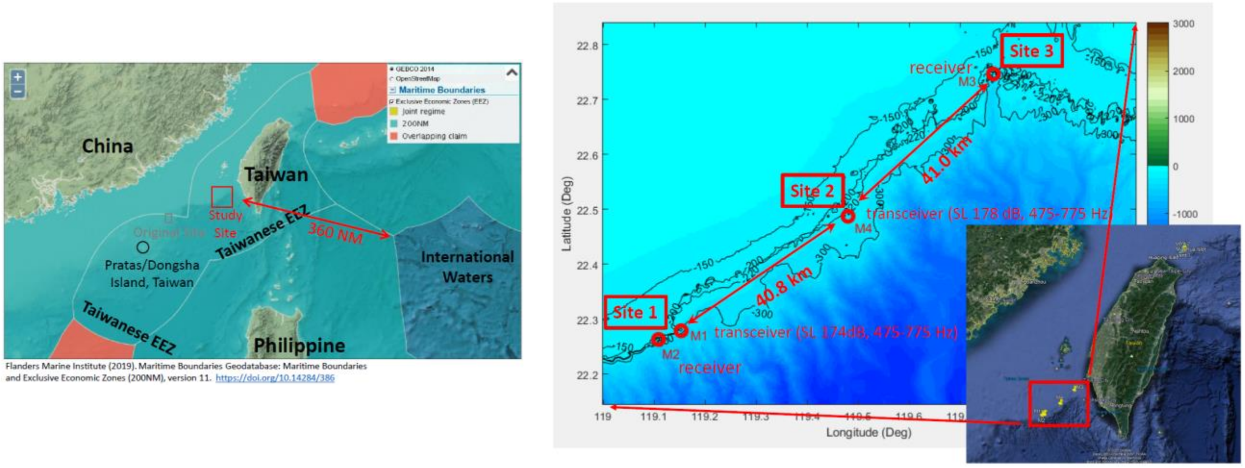

Figure 2. The location of the South China Sea (SCS) Shelf Break Acoustics Experiment. There were three study sites (see the right panel) for slope and internal wave acoustics study at Site 1, geoacoustics at Site 2 and canyon acoustics at Site 3.

OBJECTIVES

The primary scientific goal of this project is to investigate the acoustic sensitivity of ocean environmental variations in shelf break regions, with equally important goals to study their influences on acoustic localization and also on environmental characterization via inversions. Two experiments investigating the physics link between ocean environmental variability and sound propagation have been conducted: one in the South China Sea and another at the New England Shelf Break. The objectives of field work experiments include studying physical oceanographic (PO), marine geological (GEO) and biological (BIO) influences on acoustic propagation, as well as advancing real-time ocean sensing and acoustic detection and localization techniques. In short, the scientific objectives aimed in this study are listed below.

(1) Investigation of sound propagation effects due to PO, GEO and BIO features and processes.
(2) Understanding of scattering effects on seafloor and sea surface boundaries
(3) Sensitivity analysis of competing environmental factors on sound propagation.
(4) Verifying theoretical predictions and numerical modeling with field experiment data.

WORK COMPLETED AND RESULTS

The major accomplishments of this project can be catalogued into two groups: (1) numerical model development and (2) experiment data analysis.

1. High order parabolic equation (PE) sound propagation model

The high order PE solution scheme has been utilized to establish a high performance computation (HPC) model for simulating sound propagation in complex underwater environments. This modal has been also utilized in the project to analyze the experiment data by performing numerical simulations to understand the propagation physics and environmental parameter sensitivity.

2. Experiment data analyses

One of the primary project objectives is to verify theoretical predictions and numerical modeling with the New England Shelf Break Acoustics (NESBA) and SCS experiment data that the PI and his collaborators have collected in 2020 and 2021. A summary of accomplished objectives is provided below, along with the focused research topics associated with each data set.

(a) Sound propagation effects of shelfbreak fronts

The first dataset that has been analyzed was collected from the acoustic transmission experiment near and in the shelfbreak fronts during the NESBA Experiments. Analytical and computational modeling have been used to examine propagation of low-frequency (105-160 Hz) sound into the fronts. The experiment measurements and model results are shown in Figs. 3 to 5. Specifically, a Warm Core Ring-enhanced oceanic front is considered. The data was collected from an 3 hours long experimental source tow, providing spatio-temporal measurements of acoustic propagation through the front across varying geometries. Coincident oceanographic measurements are used to estimate the strong temperature gradient of the water column and 3D sound speed field. Two-dimensional (2D) adiabatic mode and full-field sound propagation models are utilized to investigate the acoustic sensitivity to the frontal structure. Then, the joint effects of acoustic ducting and bathymetric slope refraction are examined using 3D sound propagation models. Key components of the measured acoustic impulse response are captured in the 3D numerical model, and the sensitivity of low-frequency propagation to the front geometry is demonstrated. This analysis result has been published in a peer-reviewed journal by one of the project postdocs in 2022:

E. Ozanich*, G. Gawarkiewicz, and Y.-T. Lin, "Study of acoustic propagation across an oceanic front at the edge of the New England Shelf," J. Acoust. Soc. Am., vol. 152, 3756-3767 (2022). DOI:10.1121/10.0016630

(b) Canyon acoustics

There was also a canyon acoustics component in the ONR TFO SCS Experiment (see Figs. 6). The experiments were designed to study 3D focusing and defocusing effects by canyon bathymetry. A 3D PE sound propagation model consisting of realistic bathymetry and a sound speed profile measured during the experiment have been established. The 3D effects are confirmed by comparing the 3D model with a 2D model (see Figs. 6f-h). An excellent agreement between measured total signal energy on the hydrophone array and the model result has been achieve. Besides that, a sensitivity analysis on the effects of environmental parameters has also been conducted. This sensitivity study emphasizes the impacts of seafloor bathymetry and sediment properties, which may alter the strength of 3D sound reflections from canyon seafloor. This analysis result has been published in a peer-reviewed journal by one of the project postdocs in 2023:

T.-T. Chen*, **Y.-T. Lin**, and L. Y.-S. Chiu, "Impacts of seafloor characteristics on three-dimensional sound propagation in a submarine canyon," JASA Express Lett., vol. 3, 016002 (2023). DOI:10.1121/10.0016835

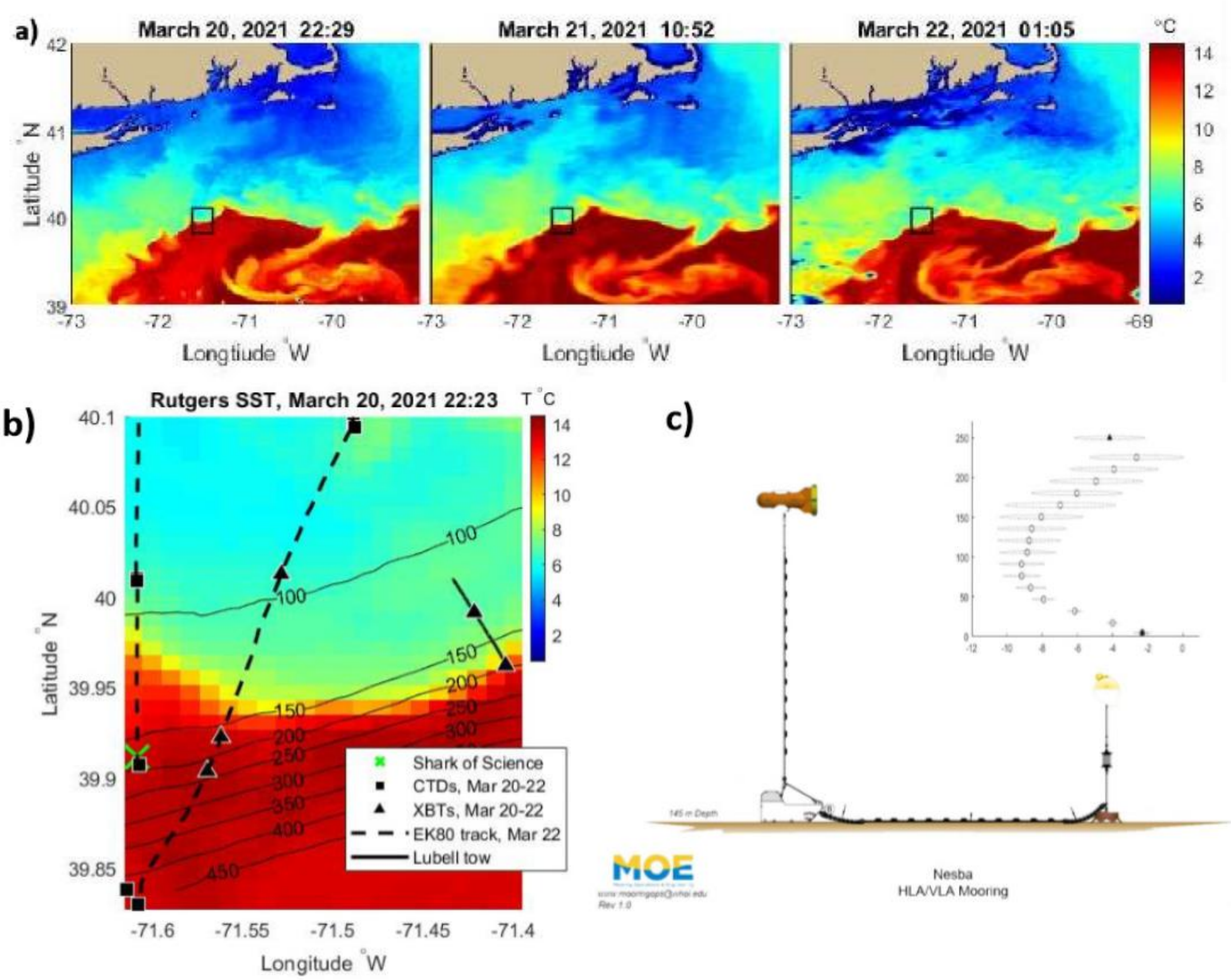

Figure 3. The Shelfbreak Front Towed Source Experiment during the NESBA Experiments. (a) Satellite images of sea surface temperature on March 20-22, 2021 indicate the evolution of Warm Core Ring water filaments and shelf water (data courtesy of Center for Ocean Observing Leadership, Dept. of Marine & Coastal Sciences, Rutgers University). The experiment region is shown with a black box. (b) Geographic locations of acoustics and oceanographic measurements from March 20-22, 2021. The source tow was conducted on March 21, 2021 01:04-04:19 GMT. (c) Diagram of the L-array mooring design in the y-z plane. An inset shows the estimated x-y positions (top down view) of the horizontal array elements in meters. Positive y is nominally magnetic North. Hydrophone positioning errors are denoted by thin-line ellipses.

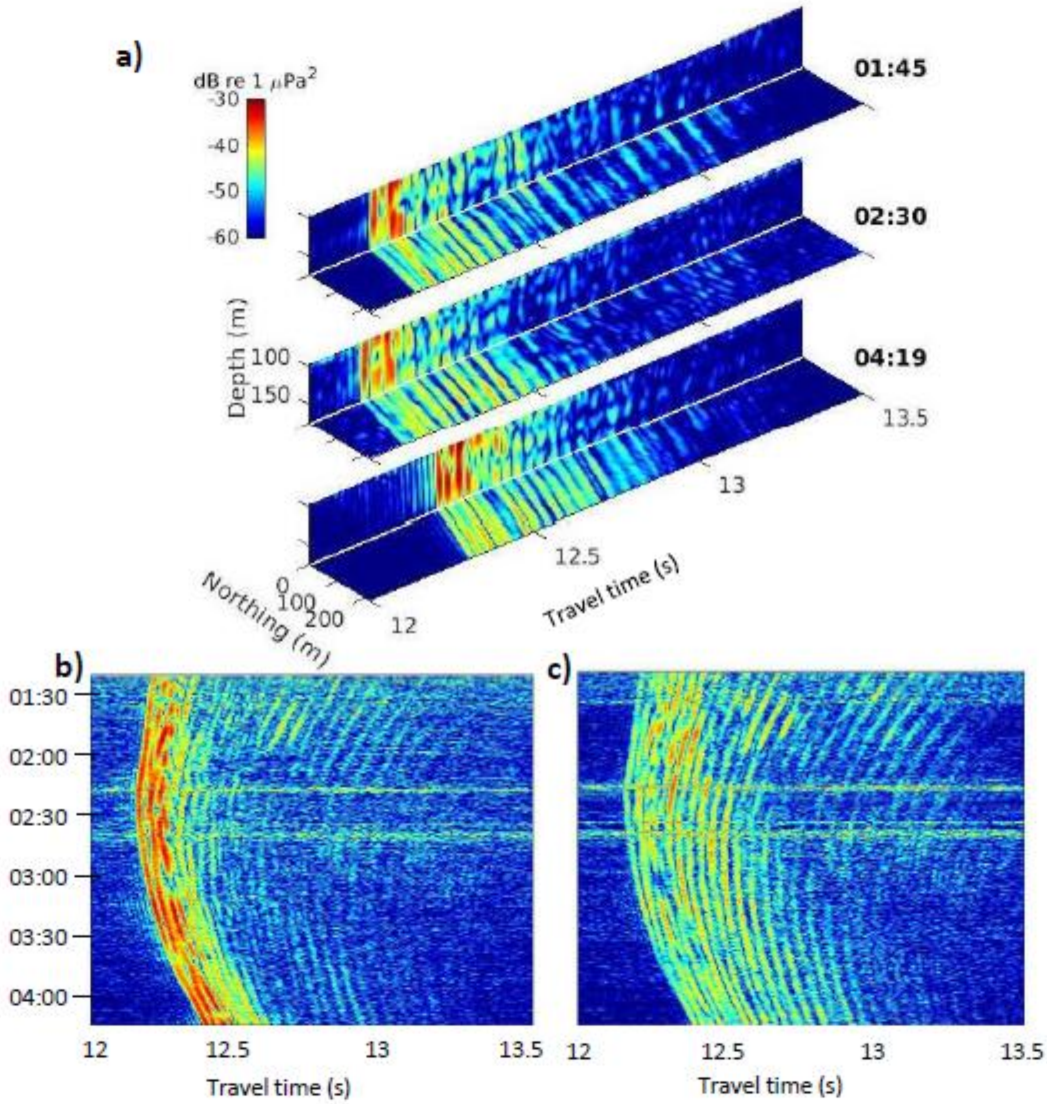

Figure 4. Example of sound propagation data collected during the Shelfbreak Front Towed Source Experiment during the NESBA Experiments. (a) Measured acoustic channel impulse responses along the vertical and horizontal L-shape array at 01:45, 02:30, and 04:19 GMT. (b) Measured impulse responses at the vertical line array (VLA) hydrophone depth 152 m over the source tow. (c) Measured impulse responses at the first horizontal line array (VLA) hydrophone closed to the VLA over the source tow.

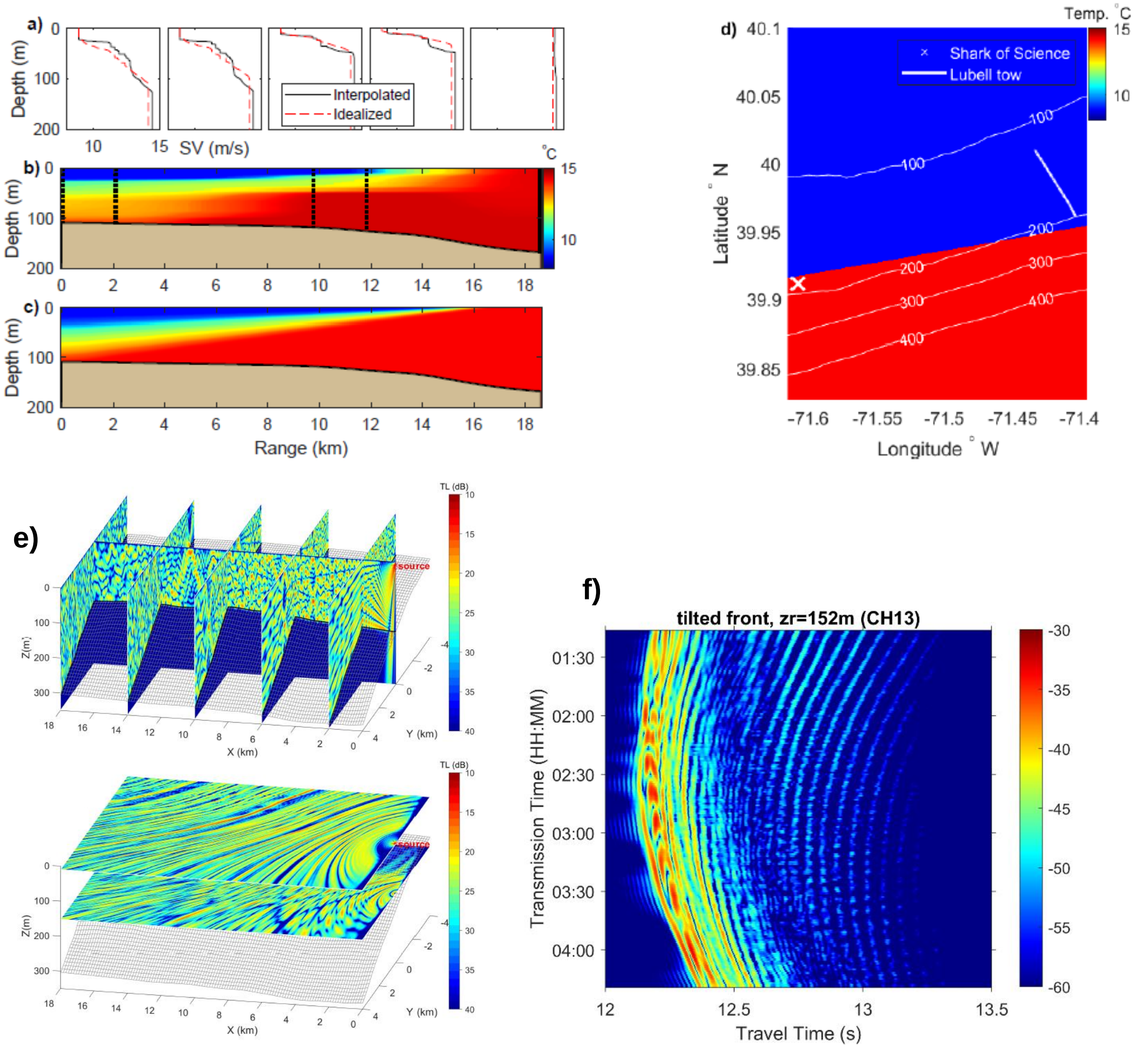

Figure 5. Numerical model results of the NESBA Shelfbreak Front Towed Source Experiment. (a) Estimated temperature vs depth at the marked ranges, for SSP interpolated from CTD and XBT measurements and the idealized linear-duct model. (b) Range-depth temperature slice along the source-receiver track using linearly interpolated oceanographic measurements projected along the source track, with CTD and XBT measurement positions are marked by vertical lines. (c) An idealized range-dependent temperature profile with linearly deepening surface duct. (d) Map of surface temperatures for the 3D idealized model. (e) Volumetric view of transmission loss at 160 Hz simulated with a 3D PE model along- and cross-sections between source and receiver, as well as at 10 m and 152 m depth. (f) Impulse response simulated at the L-array location with depth 152 m (VLA hydrophone #13) for the given 3D sound speed across the source tow using the 3D PE model. A good agreement with the data shown in Fig. 2 is found.

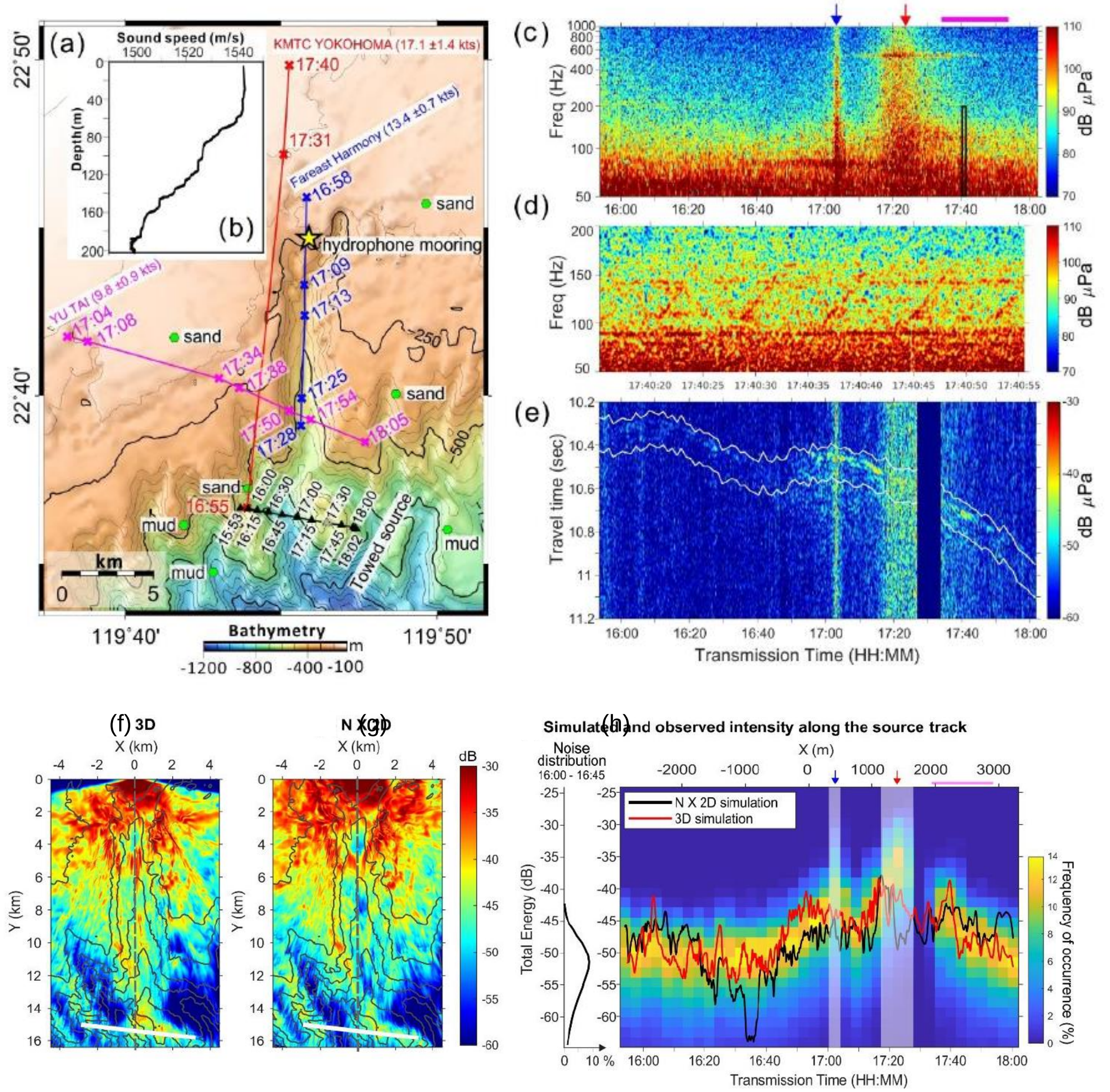

Figure 6. 3D canyon acoustic study during the TFO South China Sea Experiment. (a) The experiment layout. (b) Water sound speed profile near the hydrophone array mooring. (c) Spectrogram of received acoustic data during the entire towed source period. Two arrows and a pink line indicate the CPA of three container ships. (d) A close-up of the spectrogram within the marked window in Panel (c). (e) Coherently averaged canyon channel impulse responses across the four-channel hydrophone vertical line array during the entire towed source period. Panels (f) and (g) are the horizontal distributions of total modeled signal energy over the source frequency band (105 Hz to 160 Hz) resulted from 3D and N×2D broadband PE models, respectively. The hydrophone depth is 128 m. Panel (h) is the comparisons of the measured data (shown as energy level distributions over time) with the 3D and N×2D model results along the source track. The noise distribution during the period between 16:00 and 16:45 is shown on the side, and the average noise level was 184 -51.3 dB.

(c) Nonlinear internal wave effects

The data set collected in the SCS Shelf Break Acoustics Experiment in 2020 was analysed for studying internal wave acoustic effects, specifically on the nonlinear internal wave effects on normal incident acoustic signals. The measurements and model results are shown in Figs. 7-9. The motivation of this first study is because sonar data acquired by sub-bottom profilers and echosounder systems are widely used to estimate geoacoustic properties of marine sediments. However, the uncertainty of the seabed property estimates caused by water column variability may limit the application. In this study, the acoustic focusing and defocusing effects of nonlinear internal gravity waves on normal-incident acoustic reflection measurements is studied. The experiment data were collected in the ONR TFO South China Sea from two transceiver moorings located at two different sites (see Fig. 7), one of which contained strong nonlinear internal waves (NIWs), while another site did not. The observed reflection intensity variation at the internal wave site varied up to 10 dB (see Fig. 8). On the other hand, the bottom reflections at the other site without internal waves were stable, and a seafloor sediment sample collected there was analyzed to validate the sediment type inferred from reflection coefficients. Numerical simulations using ray-tracing and 3D PE model (see Fig. 9) confirmed the cause of this intensity fluctuation by the acoustic focusing and defocusing of NIWs. This study eventually showed that NIWs may induce a significant bias for geoacoustic property estimates from seabed reflection coefficients.

This analysis result has been published in a peer-reviewed journal by one of the project postdocs in 2023:

T.-T. Chen*, L. Y.-S. Chiu, and **Y.-T. Lin**, "Effects of nonlinear internal gravity waves on normal-incident reflection measurements of seafloor sediments," J. Acoust. Soc. Am., vol. 153, 328-337 (2023). DOI:10.1121/10.0016858

(d) Acoustic ducting by shelf water streamers

Another acoustic study was focused on sound ducting by shelf water streamers, which can produce great sound speed variability due to the Gulf Stream with increased meander amplitudes and frequency of Warm Core Ring (WCR) generation. The field observations during the NESBA experiment revealed an acoustic near-surface ducting condition induced by shelf water streamers that are related to WCRs. The field observations also revealed the subsequent disappearance of the streamer duct due to the passage of a WCR filament. These two water column conditions study highlights near-surface duct arrivals that were more dependent on water column processes, while later pulse arrivals were more closely tied to seafloor properties and structure on the New England Shelfbreak. The numerical models (see Fig. 10) have effectively been used to interpret acoustic observations in the field for two water column conditions, linking acoustic propagation with oceanographic mesoscale and submesoscale dynamics. This analysis result has been published in a peer-reviewed journal by the project research associate in 2023:

J. J. Johnson, **Y.-T. Lin**, A. E. Newhall, G. G. Gawarkiewicz, D. P. Knobles, J. D. Chaytor, and W. S. Hodgkiss, "Acoustic ducting by shelf water streamers at the New England shelfbreak," JASA Express Lett, vol. 3 (8): 086001 (2023). DOI: 10.1121/10.0020348

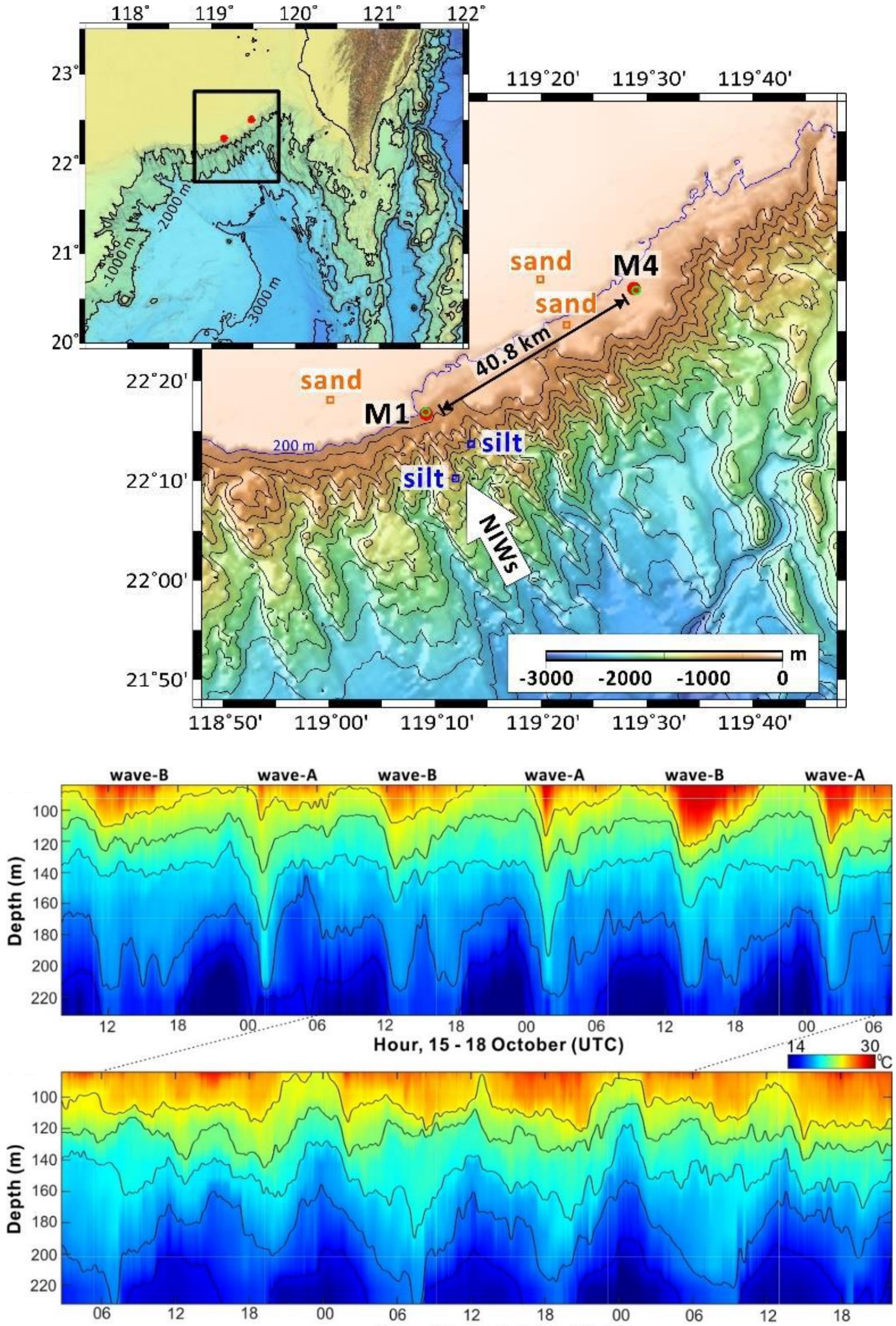

Figure 7. Study of nonlinear internal wave effects on normal incident acoustic signal during the TFO South China Sea Experiment. The top panel shows the regional map on the northeast of the SCS. Red dots indicate locations of the two moorings whose data were analyzed for studying internal wave effects on normal incident acoustic signals. Green open dots near the mooring locations are the CTD stations. The white arrow indicates the direction of NIWs. Contour interval is 200 m. The bottom two panels show that depth-Time series of temperature data at the M1 and M4 sites. The M1 site had very strong nonlinear internal waves.

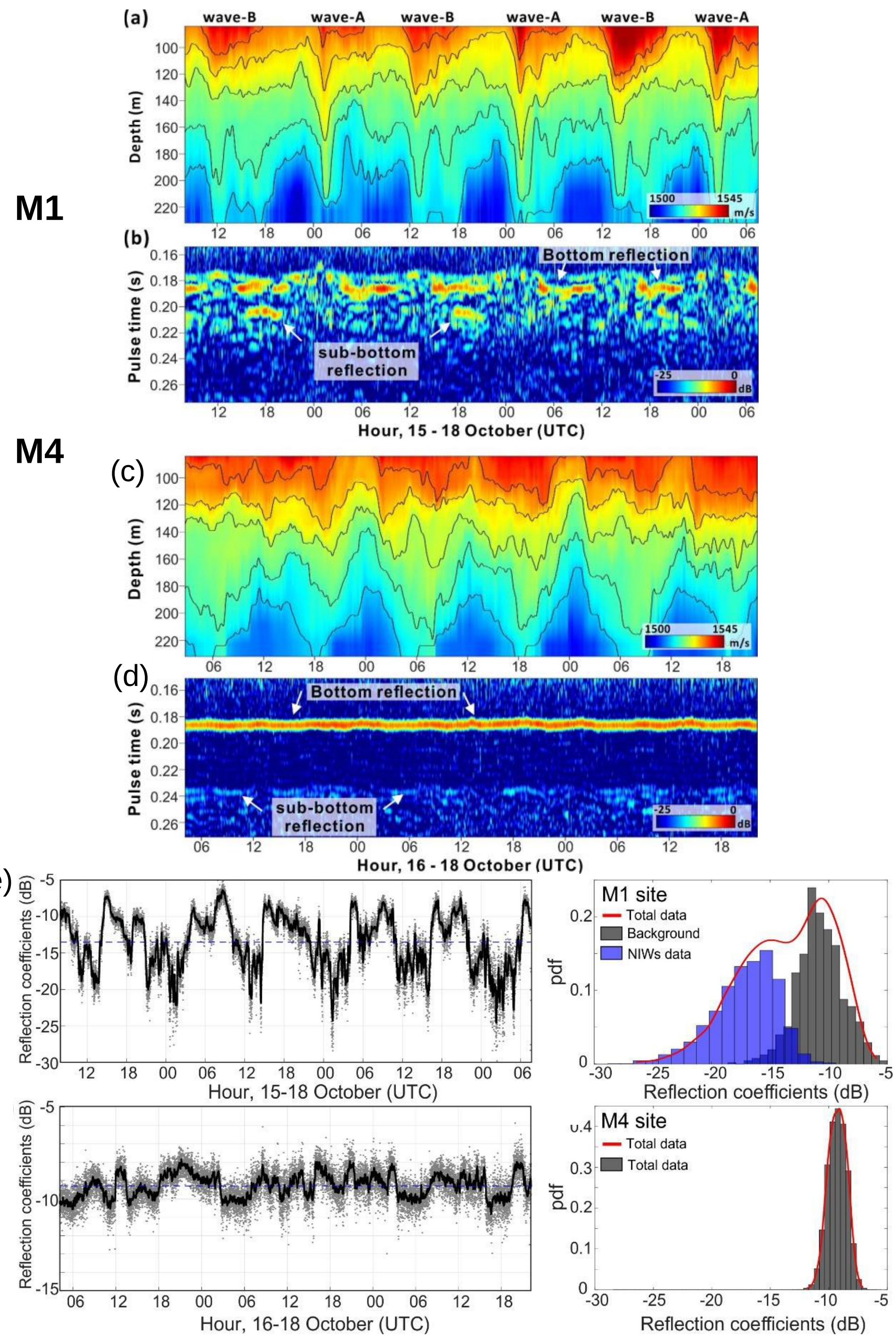

Figure 8. Measurements of nonlinear internal wave effects on normal incident acoustic signals. Panels (a) and (b) show the depth-time series of water-column sound speed profile measurements and acoustic signal reflections from the seabed at the M1 site, respectively. Panels (c) and (d) show the data at the M4 site. The acoustic signal reflections are normalized by its maximum intensity value. Panels (e) and (f) show the estimated reflection coefficients at the M1and M4 sites, respectively. Both time series of the estimates and histograms are shown.

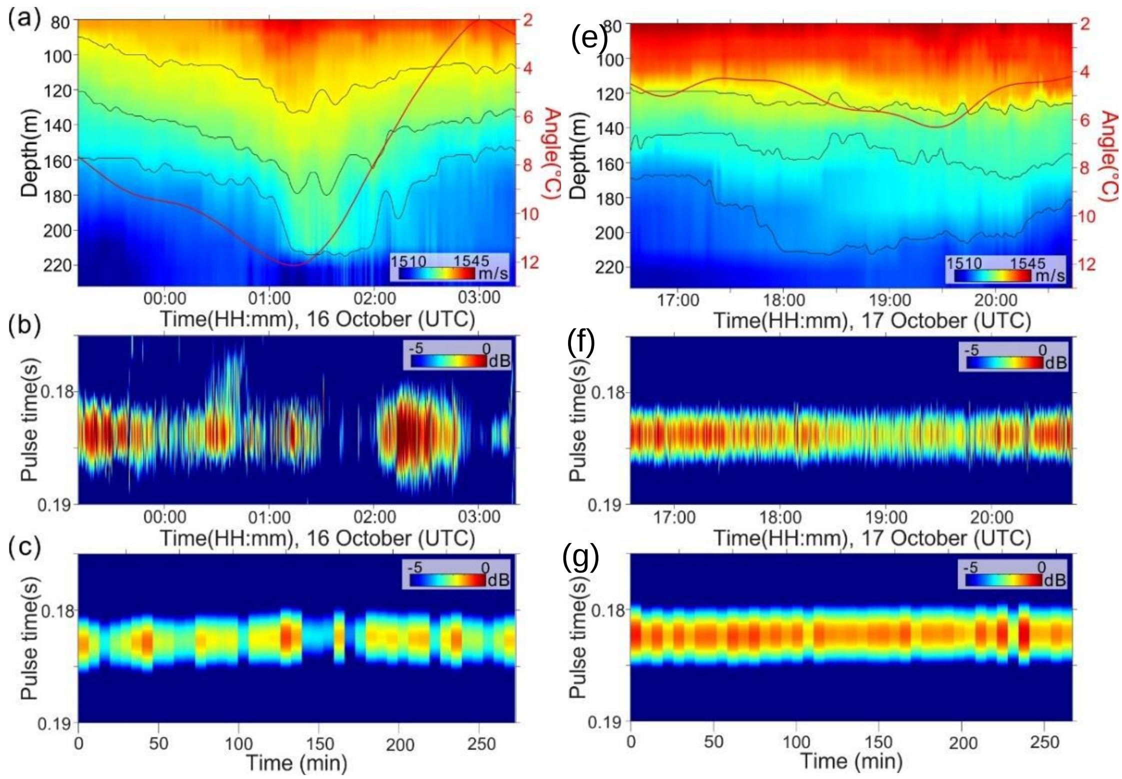

Figure 9. Numerical model results of nonlinear internal wave effects on normal incident acoustic signals. (a) Broadband frequency simulation in the wave-A field at the M1 site. A good agreement between the read data (b) and the simulated pulses (c) is observed. (e) Broadband frequency simulation at the M4 site where nonlinear internal waves were not present. A good agreement between the read data (f) and the simulated pulses (g) is observed. The red lines in the panels (a) and (e) indicate the mooring titled angle. The simulated pulses are normalized by its maximum intensity value.

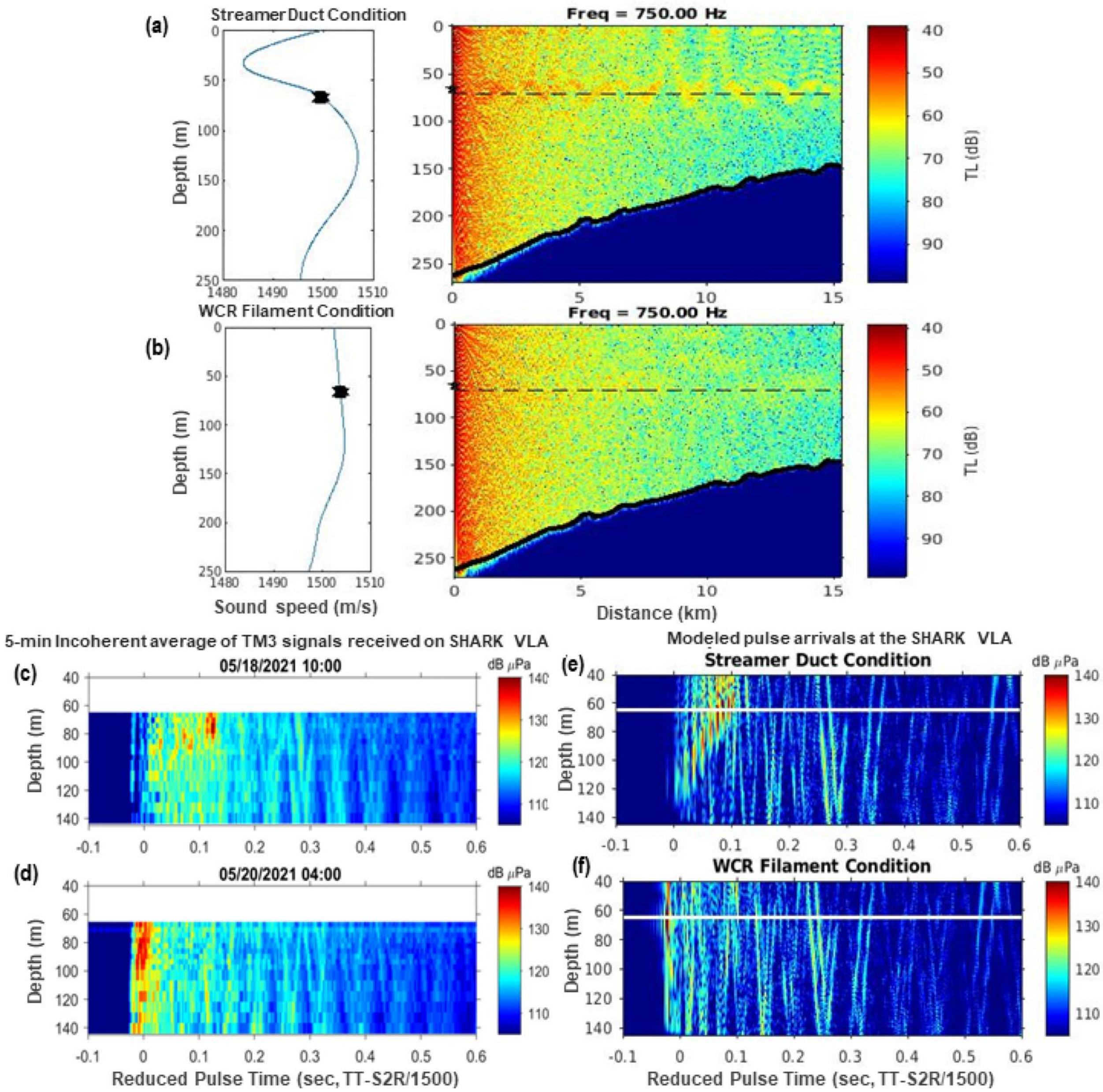

Figure 10. Upper two panels show the PE model simulation results for streamer near-surface ducting condition and WCR filament arrival condition. The average sound speed profiles are shown in the upper left panels during each water column condition, and the black dots indicate the source depth. The upper right image plots show transmission loss at 725 Hz (the center frequency of the transmitted signals in the experiment). Panels (c) and (d) depict incoherent average pulse compressed signals, and panels (e) and (f) are the broadband model results, where the white horizontal line indicates the top of the vertical line array in the experiment. One can see that the model reproduce the experiment data very well.

(e) Deep Scattering Layer acoustics

There was a transceiver array (named TM4) deployed on the slope at the 900 m isobaths in the NESBA experiment. The shipboard EK80 image showed a clear observation of a deep scattering layer, which can potentially scatter sound in the deep water. A dataset collected during an AUV mission has been used to study the Deep Scattering Layer (DSL) effect. The AUV was equipped with a 3.5 kHz sound source (2k Hz bandwidth), and the transmitted signals were received by the TM4 array (see Fig. 11). By comparing the receptions on two separate paths when the AUV were at two different depths (Fig. 11b), one can observe the DSL effect (Fig 11c). To confirm the cause of the difference in the sound propagation data was indeed by the DSL, the AUV source was sent to the NUWC Dodge Pond Acoustics Testing Facility to calibrate the transmission beampattern (see Fig. 12). Besides that, the AUV track has been thoroughly localized to obtain the best source angle to the hydrophone array. This work is the on-going doctoral dissertation research conducted by Ms. Natalie Kukshtel.

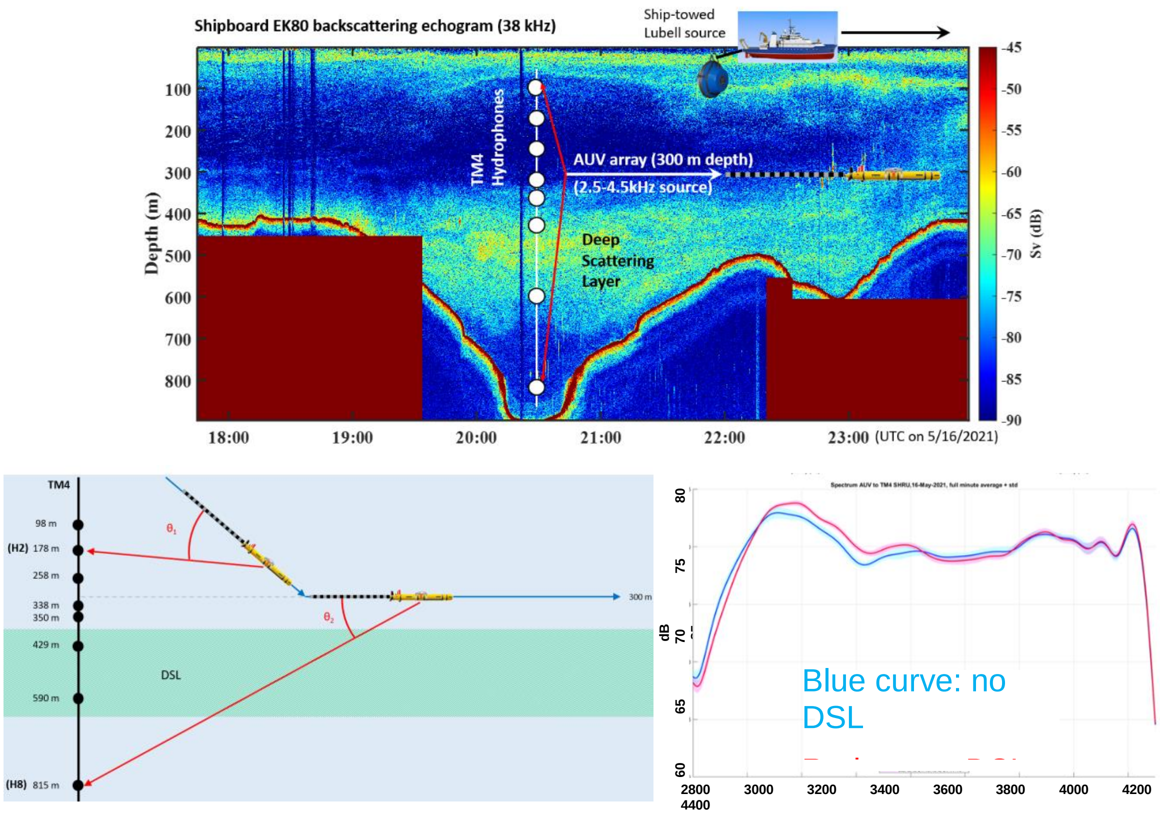

Figure 11. The Deep Scattering Layer (DSL) propagation study with an Autonomous Underwater Vehicle (AUV) during the NESBA Experiments. (a) The AUV DSL experiment layout. The AUV was equipped with a 3.5 kHz sound source (2k Hz bandwidth), and the transmitted signals were received by hydrophones on a 8-channel vertical line array (VLA) named TM4. Panel (b) shows a conceptional sketch of AUV signal propagation paths. The first one during the AUV descent to the H2 hydrophone did not pass the DSL, and the second one to the H8 hydrophone when the AUV was leveled did past through the DSL. The spectra shown in Panel (c) do show difference between these two paths, indicating possible DSL effects on sound propagation in the source frequency range (2.5-4.5 kHz).

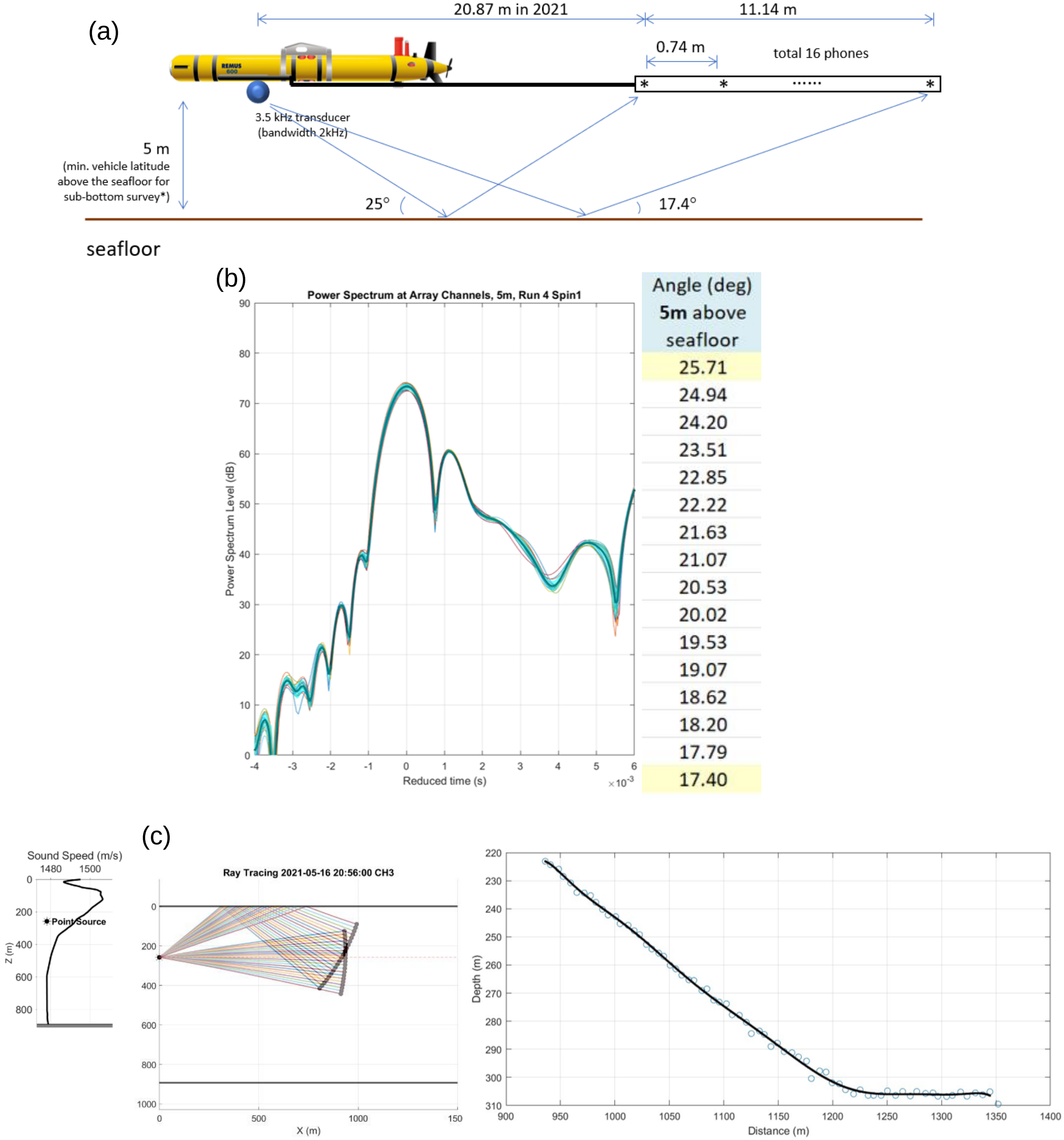

Figure 12. AUV Calibration and localization Panel (a) shows the configuration of the AUV acoustic payload. Panel (b) is the source beampattern within the launching angles to each of the towed hydrophone array channels when the AUV altitude is 5 m. Panel (c) is the AUV localization result during the DSL Propagation Experiment.

IMPACT/APPLICATIONS

The potential relevance of this work to the Navy is on increasing the capability of low- and mid-frequency sonar systems in complicated 3D acoustic environments, including long range propagation in both shallow and deep water.

RELATED PROJECTS

The experiment data was collected under an ONR TFO project entitled "Shelf Break Acoustics: An Integrated Approach for Studying Underwater Acoustic Sensitivity, Localization and Inversion," Grant # N00014-19-1-2663.

TECHNOLOGY TRANSFER

None

PARTICIPANTS

Lin, Ying-Tsong, PD/PI
Kukshtel, Natalie, Graduate Student
Chen, Tzu-Ting, Postdoctoral Researcher
Ozanich, Emma, Postdoctoral Researcher
Johnson, Jennifer, Research Associate

STUDENT

Kukshtel, Natalie

PRODUCTS

1. J. J. Johnson, Y.-T. Lin, A. E. Newhall, G. G. Gawarkiewicz, D. P. Knobles, J. D. Chaytor, and W. S. Hodgkiss, "Acoustic ducting by shelf water streamers at the New England shelfbreak," JASA Express Lett, vol. 3 (8): 086001 (2023). DOI: 10.1121/10.0020348
2. T.-T. Chen, L. Y.-S. Chiu, and Y.-T. Lin, "Effects of nonlinear internal gravity waves on normal-incident reflection measurements of seafloor sediments," J. Acoust. Soc. Am., vol. 153, 328-337 (2023). DOI:10.1121/10.0016858
3. T.-T. Chen, Y.-T. Lin, and L. Y.-S. Chiu, "Impacts of seafloor characteristics on three-dimensional sound propagation in a submarine canyon," JASA Express Lett., vol. 3, 016002 (2023). DOI:10.1121/10.0016835
4. E. Ozanich, G. Gawarkiewicz, and Y.-T. Lin, "Study of acoustic propagation across an oceanic front at the edge of the New England Shelf," J. Acoust. Soc. Am., vol. 152, 3756-3767 (2022). DOI:10.1121/10.0016630

REFERENCES

Ballard, M. S., Becker, K. M., and Goff, J. A. (2010). "Geoacoustic Inversion for the New Jersey Shelf: 3-D Sediment Model, " *IEEE J. Ocean. Eng.*, vol. 35, pp. 28-42.

Ballard, M. S., Lee, K. M., McNeese, A. R., Wilson, P. S., Chaytor, J. D., Goff, J. A., and Reed A. H. (2019). "In Situ Measurements of Compressional Wave Speed During Gravity Coring Operations in the New England Mud Patch," IEEE J. Ocean. Eng., vol. 45, pp. 26-38.

Duda, T.F., Collis, J.M., Lin, Y.-T., Newhall, A.E., Lynch, J.F., and DeFerrari, H.A. (2012). "Horizontal coherence of low-frequency fixed-path sound in a continental shelf region with internal-wave activity," *J. Acoust. Soc. Am.*, vol. 131, pp. 1782-1797.

Emerson, C., Lynch, J.F., Abbot, P., Lin, Y.-T., Duda, T.F., Gawarkiewicz, G.G., and Chen, C.-F. (2015). "Acoustic propagation uncertainty and probabilistic prediction of sonar system performance in the southern east china sea continental shelf and shelfbreak environments," *IEEE J. Ocean. Eng.*, vol. 40, pp. 1003-1017.

Lin, Y.-T., Duda, T.F., and Lynch, J.F. (2009). "Acoustic mode radiation from the termination of a truncated nonlinear internal gravity wave duct in a shallow ocean area," *J. Acoust. Soc. Am.*, vol. 126, pp. 1752-1765.

Lin, Y.-T., and Lynch, J.F. (2011). "Analytical study of the horizontal ducting of sound by an oceanic front over a slope," *J. Acoust. Soc. Am.*, vol. 131, pp. EL1-EL7.

Lin, Y.-T., Duda, T.F., Emerson, C., Gawarkiewicz, G.G., Newhall, A.E., Calder, B., Lynch, J.F., Abbot, P., Yang, Y.-J., and Jan, S. (2015) "Experimental and numerical studies of sound propagation over a submarine canyon northeast of Taiwan," *IEEE J. Ocean. Eng.*, vol. 40, pp. 237-249.

Lynch, J.F., Lin, Y.-T., Duda, T.F., and Newhall, A.E. (2010). "Acoustic Ducting, Shadowing, Refraction and Dispersion by Curved Non-Linear Internal Waves in Shallow Water," *IEEE J. Ocean. Eng.*, vol. 35, pp. 12-27.

Lynch, J.F., Emerson, C., Abbot, P.A., Gawarkiewicz, G.G., Newhall, A.E., Lin, Y.-T., and Duda, T.F. (2012). "On whether azimuthal isotropy and alongshelf translational invariance are present in low-frequency acoustic propagation along the New Jersey shelfbreak," *J. Acoust. Soc. Am.*, vol. 131, pp. 1762-1781.

Newhall, A.E., Lin, Y.-T., Grothues, T.M.. Lynch, J.F. and Gawarkiewicz, G.G. (2017). "A method of observing acoustic scattering and attenuation by fish schools using autonomous underwater vehicles," *IEEE J. Ocean. Eng.*, vol. 42, pp. 29-36.

REPORT DOCUMENTATION PAGE

1. REPORT DATE	2. REPORT TYPE	3. DATES COVERED START DATE	3. DATES COVERED END DATE
20240411	Final Research Performance Progress Report	20211001	20230930

4. TITLE AND SUBTITLE
Shelf Break Acoustics - NESBA and SCS Data Analysis

5a. CONTRACT NUMBER	5b. GRANT NUMBER	5c. PROGRAM ELEMENT NUMBER
	N00014-21-1-2959	
5d. PROJECT NUMBER	**5e. TASK NUMBER**	**5f. WORK UNIT NUMBER**

6. AUTHOR(S)
Lin, Ying-Tsong

7. PERFORMING ORGANIZATION NAME(S) AND ADDRESS(ES)
Woods Hole Oceanographic Institution
266 Woods Hole Road
Woods Hole, MA 02543-1535

8. PERFORMING ORGANIZATION REPORT NUMBER

9. SPONSORING/MONITORING AGENCY NAME(S) AND ADDRESS(ES)
Office of Naval Research, Ocean Atmosphere and Space Research Division
875 North Randolph Street
Arlington, VA 22203-1995

10. SPONSOR/MONITOR'S ACRONYM(S)
ONR

11. SPONSOR/MONITOR'S REPORT NUMBER(S)

12. DISTRIBUTION/AVAILABILITY STATEMENT
Approved for Public Release; Distribution is Unlimited

13. SUPPLEMENTARY NOTES

14. ABSTRACT
Underwater sound propagation in the ocean can be affected by a number of environmental factors, including physical oceanography, marine geology, and biology. The primary objective of the proposed work is to investigate the physics link connecting acoustics and these environmental factors, and also to verify theoretical predictions and numerical models by comparing them to field work experiment data. The ocean processes of particular interest include shelf-break fronts, thermohaline intrusions, surface mixed layers, and internal waves.

15. SUBJECT TERMS
Sound propagation, underwater acoustics, New England shelf break, South China Sea

16. SECURITY CLASSIFICATION OF: a. REPORT	b. ABSTRACT	C. THIS PAGE	17. LIMITATION OF ABSTRACT	18. NUMBER OF PAGES
U	U	U	UU	16

19a. NAME OF RESPONSIBLE PERSON	19b. PHONE NUMBER *(Include area code)*
Ying-Tsong Lin	858-534-8752

PREVIOUS EDITION IS OBSOLETE.

STANDARD FORM 298 (REV. 5/2020)
Prescribed by ANSI Std. Z39.18